Original Article

Seismic anisotropy of the upper mantle beneath Thailand: Tectonic setting constrained by shear-wave splitting analysis

Wisawet Wongwai[1], Passakorn Pananont[1*], Eric Sandvol[2], and Kevin Furlong[3]

[1] *SEIS-SCOPE, Department of Earth Sciences, Faculty of Science,*
Kasetsart University, Chatuchak, Bangkok, 10900 Thailand

[2] *Department of Geological Sciences, University of Missouri,*
Columbia, Missouri, 65211 United States of America

[3] *Department of Geosciences, The Pennsylvania State University,*
Pennsylvania, 16802 United States of America

Abstract

The tectonic setting of the lithosphere and upper mantle underneath Thailand varies and changes substantially over short distances. We have mapped these variations using shear wave splitting (SWS) analysis. We have determined the shear wave splitting fast polarization azimuth (Φ) and delay time (δt) using the grid search method with the assumption of a flat, single-layer upper-mantle anisotropy. The data set was constructed using 117 teleseismic earthquakes with magnitudes greater than 5.8, and epicentral distances between 80 and 180 degrees that occurred between 2009 and 2013, using earthquake information from USGS Comprehensive Earthquake Catalog. This resulted in 425 observations with clear P-wave arrivals, SKS, and SKKS phases. Our results show that 70% of the stations (15 of 22 stations) on the Shan-Thai terrane have N-S fast orientations and an average delay time of 0.7±0.2 seconds. 100% of the stations (14 stations) located on the Indochina terrane have dominantly E-W fast orientations and an average delay time of 0.8±0.2 seconds. This point supports the interpretation that on a lithospheric scale, Thailand consists of two major terranes.

Keywords: Thailand, tectonic setting, shear-wave splitting

1. Introduction

Southeastern Asia is built on a suite of continental blocks that include South China (Yangtze and Cathaysia), Indochina, Simao, Shan–Thai (or Sibumasu) and West Burma (Metcalfe, 2002). These blocks are separated by narrow sutures, in which dismembered ophiolites or deep-sea sediments have been observed, possibly representing remnants of different Tethyan basins (Hutchison, 1975, 1989, 1993; Sengör, 1984). Previous studies of the tectonic and geologic evolution of Thailand conclude that Thailand consists of the Shan–Thai (ST) and Indochina (IC) microcontinents or terranes welded together by the subsequently deformed Nan Suture, Figure 1(a). During the Middle Triassic, the Shan–Thai terrane sutured nearly simultaneously to Indochina and to South China, as part of the Indosinian Orogeny, with Indochina underthrusting the Shan–Thai terrane (Achache, Courtillot, & Besse, 1983; Barr & Macdonald, 1978, 1991; Bunopas, 1981; Bunopas & Vella, 1983, 1992; Chaodumrong & Burrett, 1997; Chaodumrong, Xiangdong, & Shuzhong, 2007; Charusiri, Clark, Farrar, Archibald, & Charusiri, 1993; Charusiri, Daorerk, Archibald, Hisada, & Ampaiwan, 2002; Fortey & Cocks, 1998; Hirsch, Ishida, Kozai, & Meesook, 2006; Hutchison & Charles, 2010; Konigshof *et al.*, 2012; Metcalfe, 2011, 2013). These two microcontinents are sepa-

*Corresponding author
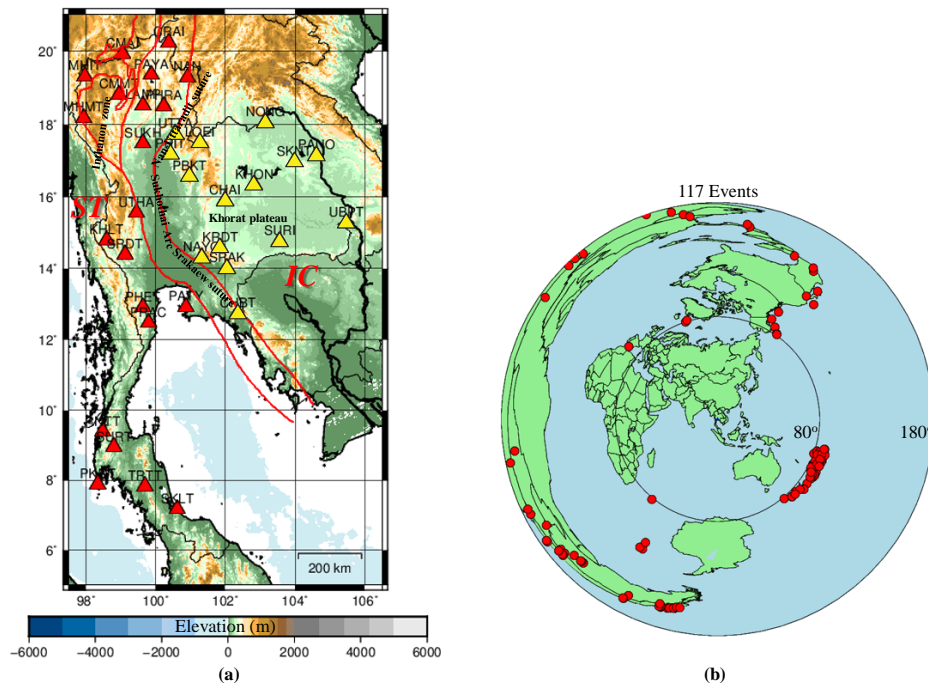Email address: fscipkp@ku.ac.th; passakorn.p@ku.th

Figure 1.   (a) Topography and tectonic setting map of Thailand with the distributions of 36 seismic stations of the Earthquake Observation Division, Thai Meteorological Department Seismic Network of which their data were used in this study. Red triangles represent stations located on Shan-Thai terrane (ST) and yellow triangles represent stations located on Indochina terrane (IC). (b) Distribution of 117 teleseismic events with epicentral distance between 80-180 degrees used in this study.

rated by the Nan suture or Nan-Uttaradit suture in the north and the Srakaeo suture in the southeast, which is a volcanic arc terrane. The Shan-Thai terranes (ST) are situated in west Yunnan in south China, eastern Myanmar, and the entire western half of Thailand and South-West Sumatra. The Indochina terrane (IC) covers south China, Laos, Vietnam, Cambodia, and the eastern half of Thailand and east Malaya (Bunopas, 1981; Bunopas & Vella, 1983; Charusiri *et al.*, 2002; Ferrari, McWilliams, Canuto, & Dubovikov, 2008; Sone & Metcalfe, 2008; Ueno & Charoentitirat, 2011), Figure 1 (a).

Several recent geophysical studies have focused on determining the crustal structure and properties of Thailand using teleseismic receiver functions. Results of these studies indicate that the crustal thickness beneath the Indochina terrane (IC) is thicker than beneath the Shan-Thai terrane (ST), varying between 33-45 km and 25-33 km, respectively. In addition, in general, the V_P/V_S ratio is relatively high (i.e. more than a typical crust value of 1.7, Paul *et al.*, 2001) in the Indochina terrane (IC) and lower (V_P/V_S ratio of 1.7 or lower) in the Shan-Thai terrane (ST) (Noisagool, Boonchaisuk, Pornsopin, & Siripunvaraporn, 2014; Tadapansawut, Chaisri, & Naunnin, 2012; Wongwai & Nuannin, 2010, 2011; Wongwai, Pananont, & Pornsopin, 2013; Yu *et al.*, 2017; Yu, Shi, & Yang, 2016;).

Yu *et al.* (2018) used teleseismic shear-wave splitting analysis (SWS) to interpret the characteristics of mantle flow beneath the Indochina peninsula. Their 409 SWS measurements using 29 regional stations (12 stations located in Thailand) show that upper mantle anisotropy beneath most of their study area is dominantly characterized by E-W orientation of the faster shear wave. They infer a mantle upwelling

as the cause of their observed azimuthal anisotropy beneath the southern part of the Peninsula. In addition of using the result of SWS measurement to characterize the mantle flow direction, it can be used to delineate the anisotropy of the upper mantle or at lithospheric scale as well since the SWS is a measurable consequence of shear waves that traverses a region with a preferred orientation of minerals either from mantle flow or a lattice preferred orientation (LPO) in the mantle (i.e. Long & Silver, 2009).

In this study, we present new SWS measurement to constrain the tectonic setting of Thailand by imaging the mantle anisotropy and identify specific 'fabric' orientations and also determine the boundaries between the different terranes at upper mantle depths. We have used 36 seismic stations operated by the Earthquake Observation Division, Thai Meteorological Department with a more spatially complete coverage of Thailand. This allows us to determine SWS behavior at a higher spatial resolution than previously possible. This work is the first step in identifying and constraining the pattern of upper mantle structure and fabric of Thailand. This will provide an important data set for future studies of what is causing the differences between the two terranes.

2. Materials and Methods

2.1 Data collection

The 36 seismic stations, Figure 1 (a), managed by the Earthquake Observation Division, Thai Meteorological Department, are equipped with three-component seismometers with frequency responses from 1s-50 Hz, 40s-50 Hz and 120s-50 Hz (Nanometrics Trillium120P, Trillium40 sensors with a

Taurus digitizer recorded continuously at 100 samples per second and Geotech KS2000 and S13 with a Smart24 digitizer recorded continuously at 50 samples per second). We analyze data from 117 teleseismic earthquakes occurring between 2009 and 2013 (48 months) with magnitudes greater than 5.8, and epicentral distances between 80 and 180 degrees from earthquake information of the United States Geological Survey Comprehensive Earthquake Catalog, producing 425 observations with clear P-wave arrivals, SKS, and SKKS phases, Figure 2 (b).

2.2 SWS measurements

The principle cause of observed seismic anisotropy of the Earth's upper mantle is produced by the preferred orientation of olivine minerals in the upper mantle, that can be produced by mantle flow or shear deformation, (Backus, 1962; Crampin, 1984; Kendall *et al.*, 2006; Nicolas & Chris tensen, 1987). The Shear wave splitting technique (SWS) has been widely adopted to use core-transiting phases such as SKS, SKKS, PKS to determine receiver-side upper mantle anisotropy (e.g., Bacon, Barnett, & Scattergood, 1980; Chang, Ferreira, Ritsema, Heijst, & Woodhouse, 2014; Lei, Xie, Fan, & Santosh, 2013; Liu & Gu, 2012; Manea, Manea, Ferrari, Orozco-Esquivel, & Kostoglodov, 2017; Nowacki, Wookey, & Kendall, 2011; Romanowicz & Wenk, 2017; Singh, Singh, & Kennett, 2015; Silver & Chan, 1991; Tommasi & Vauchez, 2015; Vauchez, Tommasi, & Mainprice, 2012; Vinnik, Ko sarev, & Makeyeva, 1984; Wu, Kuo-Chen, & McIntosh, 2014). The SKS and SKKS phases are especially well-suited

for shear wave splitting measurements because the core-mantle conversion from P (K in core) to S removes any effects from anisotropy on the source side, and produces a radially-polarized shear wave on the receiver side (Olive, Pearce, Rondenay, & Behn, 2014). A main assumption in measuring splitting parameters is that the mantle being sampled beneath a station has a coherent fabric or flow orientation on length scales that are comparable to or larger than the station spacing.

A split shear wave is defined by two parameters: the polarization direction of the first arrival phase (fast azimuth, Φ) and the time delay between the fast and slow polarizations when the shear wave travels through anisotropic materials (delay time, δt, i.e. Sandvol *et al.*, 2003). We applied the grid search method of Silver and Chan (1991) for SWS measure-ment under the assumption of single-layer anisotropy with a vertical symmetry axis. The delay time is proportional to the product of the thickness of the anisotropic layer and the strength of anisotropy. In our study we used high signal-to-noise SKS (249 phases) and SKKS (125 phases) core phases based on the AK135 velocity model (Kennett, Engdahl, & Buland, 1995) from 117 events, and 1,275 waveforms. Each waveform was analyzed in a window beginning 15 seconds before the core phase arrival and ending after one period of onset of the core phases. Each phase that displayed the elliptical horizontal particle motion indicative of shear-wave splitting was used in this study. After determining parameters that minimized the tangential component energy, we checked to insure that the corrected seismograms had an approximately linear particle motion.
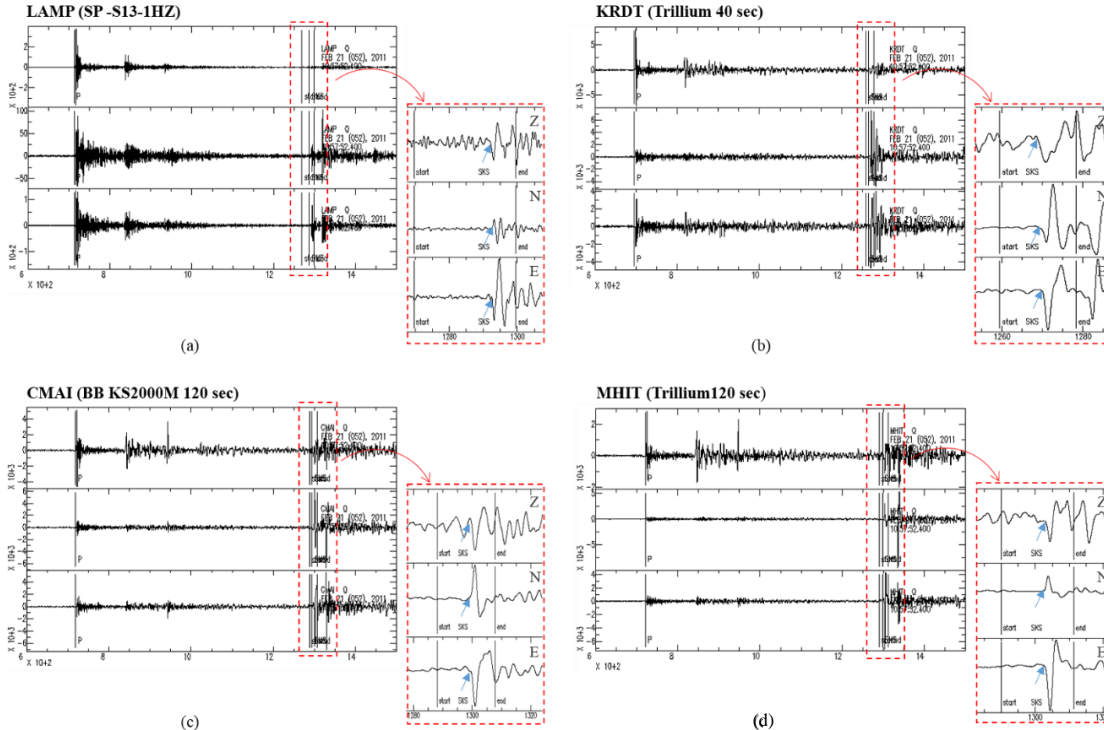

Figure 2.　Example of SKS seismic phase on 3-components teleseismic data (M 6.6, depth=545 km) occurred at South of Fiji Islands (USGS) recorded by different seismometers. (a) Station LAMP (Geotech S13: Short Period, 1HZ), (b) Station KRDT (Nanometrics Trillium40: 40s), (c) Station CMAI (Geotech KS2000M: 120s) and (d) Station MHIT (Trillium120: 120s). Note that although the S13 is a short period (1Hz) seismometer, the SKS phase is well observed.

Using the Φ estimate determined following the procedure above, the SKS wave is rotated into its fast vs. slow components, Figure 3(b). These components are time-shifted by the δt estimate to correct for the offset. This should yield very similar waveforms (possibly of opposite signs) on the corrected fast and slow components and provides a helpful diagnostic tool for measurement quality, Figure 3(c). Finally, the splitted and unsplitted (corrected) SKS waves are plotted in fast vs. slow, radial vs. transverse and east vs. north co-ordinates, Figure 3(b). The split shear wave should appear as an ellipse on all plots, Figure 3(b), and is typically plotted in map view as a bar oriented in the fast direction with length scaled by the δt estimate, Figure 3(d).

3. Results

The SWS measurement results from this study are shown in Table 1. They consist of the calculated shear wave splitting parameter at the 36 seismic stations of the Earthquake Observation Division, Thai Meteorological Department. The measurement of the fast azimuth (Φ) and delay time (δt) typically had an average errors of about $\pm 15°$ and ± 0.2 seconds, respectively (two standard deviations). The fast azimuth (Φ) results can be classified into two sets: dominantly E-W and N-S fast orientations. The first group (E-W orientation) consists of 21 stations, (CHAI, CMMT, KHON, KRDT, LOEI, NAYO, NONG, PANO, PATY, PBKT, PHET, PHIT,
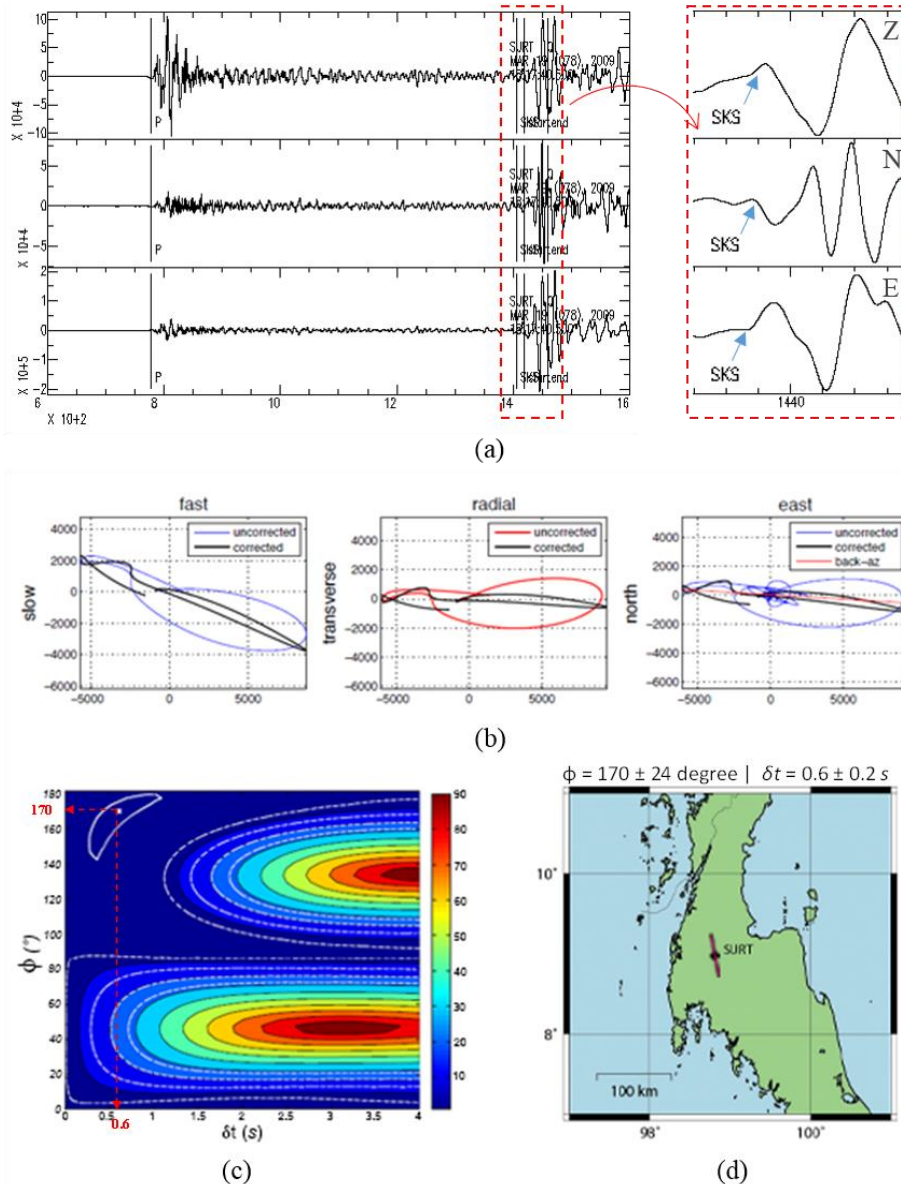

Figure 3. (a) Example of processed data recorded at station SURT with clear arrivals of SKS phases for teleseismic event (M7.9, depth = 10 km and Δ = 91.1 degrees) in the Tonga Islands Region (USGS). (b) Split and unsplit SKS waves rotated into fast vs. slow orientations (left), radial vs. transverse orientations (middle) and east vs. north orientation (right). (c) Example of an SWS modeling result for this event at SURT. Misfit as a function of orientation and delay time are contoured. Range of best fitting (minimum) results (+/-) obtained from this result. (d) Result of SWS measurements on the map.

Table 1.   Average SWS measurement results (fast direction (ϕ) and delay time (δt)) for each of the 36 seismic stations of Earthquake Observation Division, Thai Meteorological Department coverage Thailand from this analysis (* indicates the stations that are the same as those used in Yu *et al.* (2018)'s study whose results of Φ (°) and δt (s) are shown in parentheses for a comparison.

Station	Lat. (°)	Lon. (°)	Elevation (m)	Sensor	Φ (°)	δt (s)	Events
CHAI	15.902	101.986	199	SP -S13-1HZ	39 ± 24	0.9 ± 0.3	11
CHBT	12.744	102.353	198	Trillium120 sec	-18 ± 36	0.6 ± 0.3	3
CMAI*	**19.932**	**99.045**	**1,503**	BB KS2000M 120 sec	**-47 ± 7 *(137 ± 8)***	**1.2 ± 0.1 *(1.2 ± 0.1)***	**22 (11)**
CMMT*	**18.814**	**98.944**	**399**	Trillium120 sec	**80 ± 15 *(99 ± 10)***	**0.6 ± 0.1 *(1.3 ± 0.1)***	**47 (27)**
CRAI*	**20.229**	**100.373**	**357**	BB KS2000M 120 sec	**30 ± 16 *(152 ± 11)***	**1.0 ± 0.2 *(0.7 ± 0.1)***	**13 (6)**
KHLT	14.797	98.589	164	Trillium 40 sec	31 ± 23	0.6 ± 0.2	9
KHON	16.338	102.823	135	SP -S13-1HZ	-58 ± 9	0.5 ± 0.2	6
KRDT	14.591	101.844	268	Trillium 40 sec	69 ± 18	0.6 ± 0.2	14
LAMP	18.523	99.632	247	SP -S13-1HZ	-31 ± 10	0.7 ± 0.2	19
LOEI*	**17.509**	**101.264**	**306**	BB KS2000M 120 sec	**110 ± 11 *(66 ± 4)***	**1.1 ± 0.3 *(1.8 ± 0.4)***	**11 (1)**
MHIT*	**19.315**	**97.963**	**270**	Trillium120 sec	**3 ± 7 *(1 ± 19)***	**0.6 ± 0.3 *(1.3 ± 0.1)***	**12 (12)**
MHMT	18.176	97.931	200	Trillium 40 sec	-35 ± 12	0.6 ± 0.3	16
NAN	19.284	100.912	262	SP -S13-1HZ	13 ± 12	0.8 ± 0.5	19
NAYO*	**14.315**	**101.321**	**106**	BB KS2000M 120 sec	**66 ± 9 *(63 ± 7)***	**1.1 ± 0.2 *(1.1 ± 0.1)***	**10 (6)**
NONG*	**18.063**	**103.146**	**140**	BB KS2000M 120 sec	**87 ± 6 *(106 ± 11)***	**1.2 ± 0.1 *(1.2 ± 0.1)***	**13 (12)**
PANO	17.148	104.612	136	Trillium 40 sec	-75 ±90	1.2 ± 0.2	3
PATY	12.923	100.866	39	SP -S13-1HZ	91 ± 6	0.9 ± 0.2	11
PAYA	19.36	99.869	408	SP -S13-1HZ	-5 ± 6	1.1 ± 0.3	11
PBKT*	**16.573**	**100.969**	**780**	Trillium120 sec	**68 ± 14 *(59 ± 8)***	**0.6 ± 0.2 *(1.3 ± 0.0)***	**3 (28)**
PHET	12.913	99.627	101	SP -S13-1HZ	95 ± 11	0.5 ± 0.2	2
PHIT	17.189	100.417	114	SP -S13-1HZ	-80 ± 7	0.6 ± 0.1	1
PHRA*	**18.499**	**100.229**	**187**	BB KS2000M 120 sec	**88 ± 10 *(103 ± 4)***	**1.2 ± 0.3 *(1.8 ± 0.1)***	**2 (13)**
PKDT	7.891	98.334	48	Trillium 40 sec	6 ± 8	0.6 ± 0.1	20
PRAC*	**12.473**	**99.793**	**54**	BB KS2000M 120 sec	**-35 ± 13 *(92 ± 13)***	**0.8 ± 0.3 *(1.0 ± 0.1)***	**11 (13)**
RNTT	9.39	98.478	38	Trillium 40 sec	75 ± 23	0.6 ± 0.2	6
SKLT	7.176	100.616	14.5	Trillium40 sec	163 ± 27	0.5 ± 0.3	12
SKNT	16.974	103.981	255	Trillium 40 sec	81 ± 19	0.6 ± 0.2	22
SRAK	14.012	102.043	97	SP -S13-1HZ	61 ± 6	0.9 ± 0.2	9
SRDT*	**14.395**	**99.121**	**202**	Trillium 120 sec	**-41 ± 14 *(90 ± 9)***	**0.6 ± 0.4 *(0.9 ± 0.1)***	**15 (5)**
SUKH	17.482	99.631	58	SP -S13-1HZ	80 ± 6	1.0 ± 0.2	9
SURI	14.769	103.553	126	SP -S13-1HZ	52 ± 6	0.6 ± 0.1	9
SURT	8.958	98.795	32	Trillium 40 sec	170 ±24	0.6 ± 0.2	12
TRTT	7.836	99.691	62	Trillium 40 sec	34 ±21	0.6 ± 0.3	19
UBPT*	**15.277**	**105.47**	**120**	Trillium120 sec	**79 ± 21 *(79 ± 6)***	**0.6 ± 0.2 *(1.1 ± 0.1)***	**6 (5)**
UTHA	15.559	99.445	129	SP -S13-1HZ	-78 ± 4	0.8 ± 0.3	5
UTTA	17.744	100.554	63	SP -S13-1HZ	-83 ± 5	1.1 ± 0.2	12

PHRA, RNTT, SKNT, SRAK, SUKH, SURI, UBPT, UTHA, and UTTA). The N-S orientation group consists of 15 stations, (CHBT, CMAI, CRAI, KHLT, LAMP, MHIT, MHMT, NAN, PAYA, PKDT, PRAC, SKLT, SRDT, SURT, and TRTT). We found that all 15 stations of this second group with dominantly N-S directed fast orientations are located within the Shan-Thai terrane (ST). Overall 15 of the 22 stations (70%) within the Shan-Thai terrane (ST) have N-S fast orientations and their average delay time is 0.7±0.2 seconds. The 14 stations (100%) located within the Indochina terrane (IC) have dominantly E-W fast orientations and their average delay time is 0.8 ± 0.2 seconds. When comparing our result with the work of Yu *et al.*, 2018, the fast azimuth (Φ) results at most stations have approximately the same broad major trend (i.e. either north-south or east-west directions, Figure 4), except for stations PRAC and SRDT (for which we do not have a clear understanding for the reason of these discrepancies). It should be noted that although the fast azimuth (Φ) for these stations is different between the two studies, the results of the delay times for these two stations are in the same range for both studies (0.8±0.3 vs 1.0±0.1 for PRAC and 0.6±0.4 vs 0.9±0.1 for SRDT, respectively). A comparison of the delay times bet-

ween these two studies shows that when considering the error, except for MHIT, CMMT and PBKT, most of the stations have the values of the delay times falling within 30% of each other.

4. Discussion and Conclusions

Figure 4 shows the shear wave splitting parameter results (fast azimuth (Φ) and delay time (δt)) at the 36 seismic stations we used in this study. There are 22 seismic stations located within Shan-Thai terrane (ST), 15 stations or 70% have dominantly N-S fast orientations with an average delay time is 0.7±0.2 seconds. The Shan-Thai terrane (ST) also includes the Inthanon zone which is interpreted to have been the Palaeo-Tethys wedge, which overthrust the Shan-Thai terrane (ST) (Ueno, 1999; Ferrari *et al.*, 2008; Sone & Metcalfe, 2008). All of the seismic stations located within the Indochina terrane (IC) show E-W fast orientations and an average delay time of 0.8±0.2 second. The Indochina terrane (IC) in Thailand is the Khorat plateau (Takemoto *et al.*, 2009). Vertically coherent lithospheric deformation can produce lithospheric anisotropy with fast orientations parallel to the
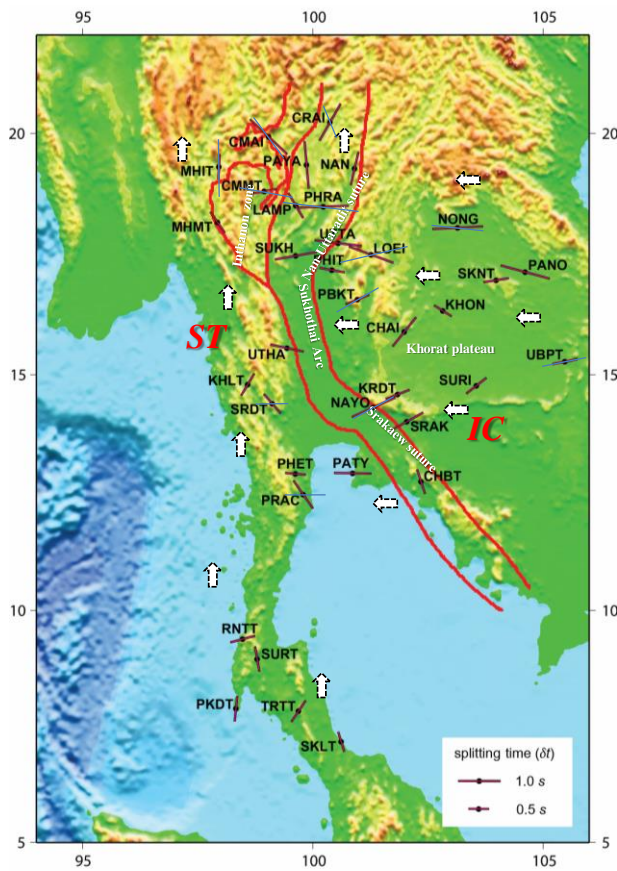
Figure 4. The SWS measurement results for all 36 seismic stations of Earthquake Observation Division, Thai Meteorological Department coverage Thailand. Red bar represent the direction of the fast orientation. White arrows represent the approximate direction of mantle flow underneath the terrane. Blue bar represent the resent Yu *et al.* (2018)'s study results for 12 stations within Thailand.

strike of the lithospheric fabric, possibly attributed to mineralogical alignment in response to regional shortening or extension (Silver, 1996; Silver & Chan, 1991). The Triassic

was a geologic period with frequent inter-plate collisions among several plates in this region, including the South China, Indochina, Simao and Shan-Thai (or Sibumasu) terranes, which there accreted onto Eurasia (Cai & Zhang, 2009); Figure 5. The Indochina and Shan-Thai (or Sibumasu) terranes are interpreted to be volcanic arc terranes (Nan suture or Nan-Uttaradit suture in the north and the Srakaeo suture in the southeast (Bunopas, 1981; Bunopas & Vella, 1983; Cha rusiri *et al.*, 2002; Ferrari *et al.*, 2008; Sone & Metcalfe, 2008; Ueno & Charoentitirat, 2011). Subduction associated with terrane accretion in this area, together with the Pacific subduction to the east during the Mesozoic could be a cause for the apparent different mineral orientations of the mantle beneath Thailand that we have observed in our SWS analysis.

Acknowledgements

References

Achache, J., Courtillot, V., & Besse, J. (1983). Paleomagnetic constraints on the late Cretaceous and Cenozoic tectonics of Southeastern Asia. *Earth and Planetary Science Letters, 63*, 123–136. doi:10.1016/0012-821 X(83)90028-6

Backus, G. E. (1962). Long-wave elastic anisotropy produced by horizontal layering. *Journal of Geophysical Research, 67*, 4427

Bacon, D. J., Barnett, D. M., & Scattergood, R. O. (1980). Anisotropic continuum theory of lattice defects. *Progress in Materials Science, 23*, 51-262.

Barr, S., & Macdonald, A. (1978). Geochemistry and petrogenesis of late Cenozoic alkaline basalts of Thailand. *Bulletin of the Geological Society of Malaysia, 10*, 25–52

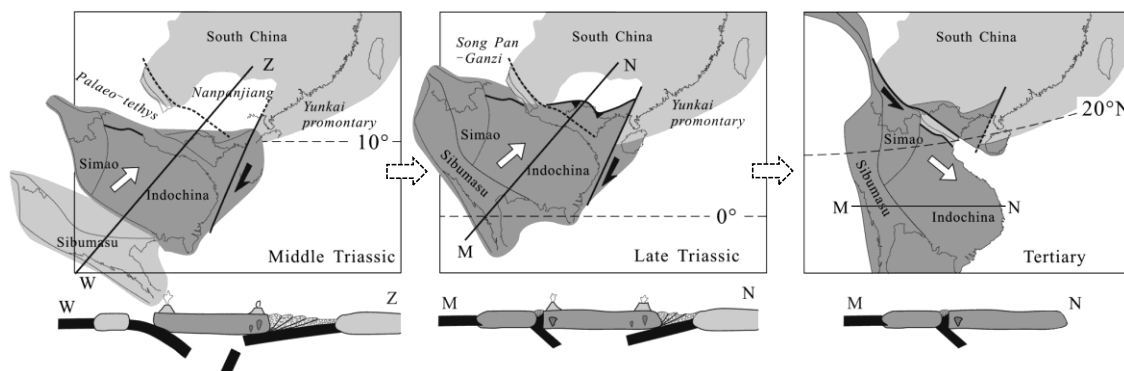Figure 5. Sketch of evolutional maps of southeastern Asia, showing the relative positions of Shan Thai (Sibumasu), Indochina and South China terranes since the Middle Triassic proposed by Cai and Zhang (2009) which suggests that the Shan Thai and Indochina were not the same terranes. This idea is supported by results of the SWS analysis in this work that indicate different SWS result among these terranes.

Barr, S., & Macdonald, A. (1991). Toward a late Paleozoic-early Mesozoic tectonic model for Thailand. *Journal of Thai Geosciences, 1*, 11–12.

Bunopas, S. (1981). Paleogeographic history of western Thai land and adjacent pets of Southeast Asia-A plate tectonics interpretation. Reprinted as Bangkok Department Mineral Resource Geological Survey Paper 2, Victoria University of Wellington, New Zealand.

Bunopas, S., & Vella, P. (1983). Tectonic and geologic evolution of Thailand. *Proceeding of the Workshop on Stratigraphic Correlation of Thailand and Malaysia* (pp. 307–322). Songkhla, Thailand.

Bunopas, S., & Vella, P. (1992). Geotectonics and geologic evolution of Thailand. *Proceeding of National Conference on "Geologic Resources of Thailand: Potential for Future Development"* (pp. 209–229). Bangkok, Thailand: Department of Mineral Resources.

Cai, J. X., & Zhang, K. J. (2009). A new model for the Indochina and South China collision during the Late Permian to the Middle Triassic. *Tectonophysics, 467*, 35–43.

Chang, S. J., Ferreira, A. M., Ritsema, J., Heijst H. J., & Woodhouse, J. H. (2014). Global radially anisotropic mantle structure from multiple datasets: A review, current challenges, and outlook. *Tectonophysics, 617*, 1-19.

Chaodumrong, P., & Burrett, C. (1997). Early Late Triassic continental colliding between the Shan-Thai and Indochina terranes as indicated by occurrence of fan delta redbeds of Pha Daeng Formation, central north Thailand. *Proceedings of the International Conference on Stratigraphy and Tectonic Evolution of Southeast Asia and the South Pacific* (pp. 143–157). Bangkok, Thailand.

Chaodumrong, P., Xiangdong, W., & Shuzhong, S. (2007). Permian lithostratigraphy of the Shan-Thai terrane in Thailand: Revision of the Kaeng Krachan and Ratburi Groups. *Proceedings of the GEOTHAI'07 International Conference of Geology of Thailand: Towards Sustainable Development and Sufficiency Economy* (pp. 229–236). Bangkok, Thailand: Department of Mineral Resources &Nanjing, China: Nanjing Institute of Geology and Palaeontology, Nanjing.

Charusiri, P., Clark, A., Farrar, E., Archibald, D., & Charusiri, B. (1993). Granite belts in Thailand: Evidence from the 40Ar/39Ar geochronological and geological syntheses. *Journal of Southeast Asian Earth Sciences, 8*, 127–136.

Charusiri, P., Daorerk, V., Archibald, D., Hisada, K., & Ampaiwan, T. (2002). Geotectonic evolution of Thailand: A new synthesis. *Journal of the Geological Society of Thailand, 1*, 1–20.

Crampin, S. (1984). Effective anisotropic elastic constants for wave propagation through cracked solids. *Geophysical Journal of the Royal Astronomical Society, 76*, 135-145.

Ferrari, R., McWilliams, J. C., Canuto, V. M., & Dubovikov, M. (2008). Parameterization of eddy fluxes near oceanic boundaries. *Journal of Climate - American Meteorological Society, 31*, 2770-2789. doi:10.1175/2007JCLI1510.1

Fortey, R. A., & Cocks, L. R. M. (1998). Biogeography and palaeogeography of the Sibumasu terrane in the Ordovician: A review. Biogeography and geological evolution of SE Asia, 43-56. In R. Hall, & J. D. Holloway(Eds.), *Biogeography and Geological Evolution of SE Asia*. Leiden, The Netherlands: Backhuys. doi:10.1002/mmnz.20000760119

Hirsch, F., Ishida, K., Kozai, T., & Meesook, A. (2006). The welding of Shan-Thai. *Geosciences Journal, 10*(3), 195–204. doi:10.1007/BF02910364

Hutchison, C. S. (1975). Ophiolites in Southeast Asia. *Geological Society of America Bulletin, 86*(6), 797–806

Hutchison, C. S. (1989). The Paleotethyan realm and Indosinian orogenic system of Southeast Asia. In A.M.C. Sengör (Ed.), *Tectonic Evolution of the Tethyan region. NATO ASI Series C*(Vol. 259 pp. 585–643). Dordrecht, The Netherlands: Kluwer.

Hutchison, C. S. (1993). Gondwana and Cathaysian blocks, Paleotethys sutures and Cenozoic tectonics in southeast Asia. *Geologische Rundschau, 82*, 388–405.

Hutchison, S., & Charles, A. (2010). Oroclines and paleomagnetism in Borneo and South-East Asia. *Tectonophysics, 496*(2010), 53-67.

Kendall, J., Pilidou, S., Keir, D., Bastow, I., Stuart, G., & Ayele, A. (2006). Mantle upwellings, melt migration and magma assisted rifting in Africa: Insights from seismic anisotropy. In G. Yirgu, C. J. Ebinger, & P. K. H. Maguire (Eds.), *Structure and evolution of the rift systems within the Afar volcanic province, Northeast Africa* (pp. 57-74).

Kennett, B. L. N., Engdahl, E. R., & Buland, R. (1995). Constraints on seismic velocities in the Earth from traveltimes. *Geophysical Journal International, 122*, 108-124.

Konigshof, P., Savage, N. M., Lutat, P., Sardsud, A., Dopieralska, J., Belka, Z., & Racki, G. (2012). Late Devonian sedimentary record of the Paleotethys Ocean – The Mae Sariang section, northwestern Thailand. *Journal of Asian Earth Sciences, 52*, 146–157

Lei, J., Xie, F., Fan, Q., & Santosh, M. (2013). Seismic imaging of the deep structure under the Chinese volcanoes: An overview. *Physics of the Earth and Planetary Interiors, 224*, 104-123.

Liu, Q., & Gu, Y. J. (2012). Seismic imaging: From classical to adjoint tomography. *Tectonophysics, 566–567*, 31-66.

Long, M. D., & Silver, P. G. (2009). Shear wave splitting and mantle anisotropy: Measurements, interpretations, and new directions. *Surveys in Geophysics, 30*, 407–461. doi:10.1007/s10712-009-9075-1

Manea, V. C., Manea, M., Ferrari, L., Orozco-Esquivel, T., & Kostoglodov, V. (2017). A review of the geodynamic evolution of flat slab subduction in Mexico, Peru, and Chile. *Tectonophysics, 695*, 27-52.

Metcalfe, I. (2002). Permian tectonic framework and paleogeography of SE Asia. *Journal of Asian Earth Sciences, 20*, 551–566.

Metcalfe, I. (2011). Tectonic framework and Phanerozoic evolution of Sundaland. *Gondwana Research. 19*(1), 3–21. doi:10.1016/j.gr.2010.02.016

Metcalfe, I. (2013). Tectonic evolution of the Malay Peninsula. *Journal of Asian Earth Science, 76*, 195–213. doi:10.1016/j.jseaes.2012.12.011

Nicolas, A., & Christensen, N. I. (1987). Formation of anisotropy in upper mantle peridotites – A review. In K. Fuchs & C. Froideveaux (Eds.), *'Composition structure and dynamics of the lithosphere asthenosphere system', AGU* (pp. 111-123). Washington, DC.

Noisagool, S., Boonchaisuk, S., Pornsopin, P., & Siripun varaporn, W. (2014). Thailand's crustal properties from tele-seismic receiver function studies. *Tectonophysics, 632*, 64–75.

Nowacki, A., Wookey, J., & Kendall J. M. (2011). New advances in using seismic anisotropy, mineral physics and geodynamics to understand deformation in the lowermost mantle. *Journal of Geodynamics, 52*(3–4), 205-228.

Olive, J. A., Pearce, F., Rondenay, S., & Behn, M. D. (2014). Pronounced zonation of seismic anisotropy in the western hellenic subduction zone and its geodynamic significance. *Earth and Planetary Science Letters, 391*, 100–109.

Paul, A., Cattaneo, M., Thouvenot, F., Spallarossa, D., Bethoux, N., & Frechet, J. (2001). A three-dimensional crustal velocity model of the southwestern Alps from local earthquake tomography. *Journal of Geophysical Research, 106*(B9), 19,367-19,389.

Romanowicz, B. & Wenk, H. R. (2017). Anisotropy in the deep Earth. *Physics of the Earth and Planetary Interiors, 269*, 58-90.

Sandvol, E., Turkelli, N., Zor, E., Gok, R., Bekler, T., Gurbuz, C., Seber, D., . . . Barazangi, M. (2003). Shear wave splitting in a young continent-continent collision: An example from eastern Turkey. *Geophysical Research Letters, 30*(24).

Sengör, A. M. C. (1984). The Cimmeride orogenic system and the tectonics of Eurasia. *Special Papers – Geological Society of America, 195*.

Silver, P. G. (1996). Seismic anisotropy beneath the continents: Probing the depths of geology. *Annual Review of Earth and Planetary Sciences, 24*(1), 385–432. doi:10.1146/annurev.earth.24.1.385

Silver, P. G., & Chan, W. W. (1991). Shear wave splitting and subcontinental mantle deformation. *Journal of Geophysical Research, 96*(B10), 16,429-16,454.

Singh, A., Singh, C., & Kennett, B. L. N. (2015). A review of crust and upper mantle structure beneath the Indian subcontinent. *Tectonophysics, 644–645*, 1-21.

Sone, M., & Metcalfe, I. (2008). Parallel Tethyan Sutures in mainland SE Asia: New insights for Palaeo-Tethys closure. *Compte Rendus Geoscience, 340*, 166–179.

Tadapansawut, T., Chaisri, S., & Naunnin, P. (2012). Thailand crustal thickness estimate using joint inversion of surface wave dispersion and receiver function. *Proceedings of the 6th International Conference on Applied Geophysics*. Kanchanaburi, Thailand.

Takemoto, K., Sato, S., Chanthavichith, K., Inthavong, T., Inokuchi, H., Fujihara, M., . . . Otofuji, Y. (2009). Tectonic deformation of the Indochina Peninsula recorded in the Mesozoic palaeomagnetic results. *Geophysical Journal International, 179*, 97–111. doi:10.1111/j.1365-246X.2009.04274.x

Tommasi, A., & Vauchez, A. (2015). Heterogeneity and anisotropy in the lithospheric mantle. *Tectonophysics, 661*, 11-37.

Ueno, K. (1999). Gondowana/Tethys divide in East Asia: Solution from Late Paleozoic foraminiferal Paleobiogeography. *Shallow Tethys, 5*, 45–54.

Ueno, K., & Charoentitirat, T. (2011). Carboniferous and Permian. In M. F. Ridd, A. J. Barber, & M. J. Crow (Eds.), *The Geology of Thailand* (pp. 71–136). City, England: Geological Society of London

U.S. Geological Survey. (September 1, 2013), Comprehensive earthquake catalog, Retrieved from http://earth quake.usgs.gov

Vauchez, A., Tommasi, A., & Mainprice, D. (2012). Faults (shear zones) in the Earth's mantle. *Tectonophysics, 558–559*, 1-27.

Vinnik, L. P., Kosarev, G. L., & Makeyeva, L. I. (1984). Anisotropiya litosfery po nablyudeniyam voln SKS and SKKS, Dokl. Akad. Nauk USSR 278, 1335-1339

Wongwai, W., & Nuannin, P. (2010). Crustal thickness of Thailand. *Proceedings of the 5th International Conference on Applied Geophysics: Geological Resources-Natural Hazards-Climate Change*, 11-13 November 2010, Phuket, Thailand

Wongwai, W., & Nuannin, P. (2011). The crustal thickness of Thailand by teleseismic receiver functions. (Master's thesis, Prince of Songkhla University, Songkhla, Thailand). Retrieved from https://opac.psu.ac.th/ BibDetail.aspx?bibno=351570

Wongwai, W., Pananont, P., & Pornsopin, P. (2013). Teleseismic receiver functions study of the crustal thickness underneath Thailand. *American Geophysical Union, Fall Meeting 2013*, Abstract ID. S33F-03.

Wu, F. T., Kuo-Chen, H., & McIntosh, K. D. (2014). Subsurface imaging, TAIGER experiments and tectonic models of Taiwan. *Journal of Asian Earth Sciences, 90*, 173-208.

Yu, C., Shi, X., & Yang, X. (2016). Deep thermal structure of Southeast Asia constrained by S-velocity data. *Marine Geophysical Research, 38*, 341. doi:10.10 07/s11001-017-9311-x

Yu, Y., Hungab, T., Yang, T., Xue, M., Liu, K., & Gaod, S. (2017). Lateral variations of crustal structure beneath the Indochina Peninsula. *Tectonophysics, 712–713*, 193-199. doi:10.1016/j.tecto.2017.05.023

Yu, Y., Gao, S. S., Liu, K. H., Yang, T., Xue, M., Le, K. P., & Gao, J. (2018). Characteristics of the mantle flow system beneath the Indochina Peninsula revealed by teleseismic shear wave splitting analysis. *Geochemistry, Geophysics, Geosystems, 19*. doi:10. 1029/2018GC007474